Cavities and Channels in Electrides

James L. Dye,*,† Michael J. Wagner,†,‡ Gregor Overney,†,§ Rui H. Huang,† Tibor F. Nagy,⊥ and David Tománek⊥

Contribution from the Departments of Chemistry and Physics/Astronomy and Center for Fundamental Materials Research, Michigan State University, East Lansing, Michigan 48824-1322

Received February 20, 1996. Revised Manuscript Received June 4, 1996[⊗]

Abstract: The three-dimensional geometries of cavities and channels in four electrides are determined in detail with the aid of computer graphics methods. Previous theoretical and experimental studies support the view that electrons are trapped in cavities and interact through connecting channels. The magnetic coupling constants and the dimensionalities of the magnetic interactions are consistent in all cases with the cavity and channel structures of electrides. By combining structural information and theory, it may be possible to describe the overall electronic properties of electrides with a model of an electron gas in a complex "plumber's nightmare box" whose geometry is given by the cavity and channel structures.

Introduction

Electrides are crystalline solids with the positive charges on complexed alkali metal cations balanced by an equal number of trapped electrons. Five electride structures show the common feature of one cavity per electron with diameters from 3.7 to 4.8 Å, produced by close-packing of the large (8- to 10-Å diameter) complexed cations. Yet, in spite of this similarity, the magnetic, optical, and electronic properties differ significantly from one electride to another. Recent theoretical studies support a picture in which the excess electron density tends to occupy the empty cavities and channels and to avoid the regions containing the closed shell crown ether or cryptand complexes of the alkali cations. We have used computer graphics techniques to easily determine the dimensions and structures of cavities and channels in electrides of known crystal structure. In this paper, we illustrate the cavity and channel structures of five electrides, and show the relationship of the structures to their magnetic dimensionalities and coupling constants.

Nature of Electrides. The crystal structures and properties of electrides have been described in a number of research[1−4] and review[5−10] publications. Electrides are prepared by crystallization from solutions of alkali metals and crown ether or cryptand complexants in aprotic solvent mixtures such as dimethyl ether−trimethylamine. The solution stoichiometry is adjusted to produce mainly M^+L_n and e^-_{solv}, in which L is the complexant and $n = 1$ (cryptands) or 2 (crown ethers). One electride has a mixed crown cation.[4,11]

A critical question is, "Where are the 'excess' electrons in electrides?" X-ray diffraction is no *direct* help, since the expected signal from a diffuse single electron is below the noise level. Yet the following experimental properties indicate that the bulk of the electron density is located in the otherwise empty anionic sites.

1. The complexed cation structures are essentially the same as those of salts with the same complexed cation and "ordinary" anions such as iodide, perchlorate, etc. The cation-to-oxygen distances are nearly anion independent, even when this "anion" is an electron! Thus, little excess electron population exists between the cations and the oxygen atoms of the complexant. Indeed, the thermodynamic driving force for complexation is the interaction of the cation's positive charge with lone pairs on oxygen. Neutralization of this charge would inhibit complexation.

2. Each of the first three electrides described here has an alkalide counterpart with similar local structure but with alkali metal *anions* in the cavities, suggesting that trapped electrons can serve as the anions.

3. The ^{133}Cs NMR Knight shift shows that the unpaired electron density at Cs^+ in three electrides is at least three orders of magnitude smaller than that in the cesium atom.[2,4,12] This implies a very small unpaired electron density in the 6s cesium orbital.

4. Electron paramagnetic resonance (EPR) studies of defect electorns in alkalides demonstrate that most are trapped at "empty" anionic sites.[13] The EPR spectra of defect electrons in Cs^+ (18-crown-6)$_2Na^-$ and of the isostructural electride, Cs^+-(18-crown-6)$_2e^-$ are very similar, implying the same trapping geometry.[14]

5. Pairwise trapping of K^- as K_2^{2-} occurs in K^+-(cryptand[2.2.2])K^-, with K^- to K^- distances of only 4.9 Å.[3,15]

* To whom correspondence should be addressed.
† Department of Chemistry, Michigan State University.
‡ Current address: Department of Chemistry, Massachusetts Institute of Technology, 77 Massachusetts Ave., Cambridge, MA 02139.
§ Current address: Room 2C-547, ATT Bell Laboratories, Murray Hill, NJ 07974-0636.
⊥ Department of Physical/Astronomy, Michigan State Univerity.
⊗ Abstract published in *Advance ACS Abstracts,* July 15, 1996.
(1) Dawes, S. B.; Ward, D. L.; Huang, R. H.; Dye, J. L. *J. Am. Chem. Soc.* **1986**, *108*, 3534−3535.
(2) Dawes, S. B.; Eglin, J. L.; Moeggenborg, K. J.; Kim, J.; Dye, J. L. *J. Am. Chem. Soc.* **1991**, *113*, 1605−1609.
(3) Huang, R. H.; Faber, M. K.; Moeggenborg, K. J.; Ward, D. L.; Dye, J. L. *Nature* **1988**, *331*, 599−601.
(4) Wagner, M. J.; Huang, R. H.; Eglin, J. L.; Dye, J. L. *Nature* **1994**, *368*, 726−729.
(5) Dye, J. L. *Sci. Am.* **1987**, *257*, 66−75.
(6) Dye, J. L.; DeBacker, M. G. *Annu. Rev. Phys. Chem.* **1987**, *38*, 271−301.
(7) Dye, J. L. *Science* **1990**, *247*, 663−668.
(8) Dye, J. L. In *Metals in Solution, Journal de Physique IV, Colloque C5*; Damay, P., Leclerq, F., Eds.; Les Editions de Physique: Les Ulis, France, 1991; Vol. 1; pp 259−282.
(9) Dye, J. L. *Chemtracts−Inorg. Chem.* **1993**, *5*, 243−270.
(10) Wagner, M. J.; Dye, J. L. *Annu. Rev. Mater. Sci.* **1993**, *23*, 223−253.
(11) Wagner, M. J.; Dye, J. L. *J. Solid State Chem.* **1995**, *117*, 309−317.
(12) Dawes, S. B.; Ellaboudy, A. S.; Dye, J. L. *J. Am. Chem. Soc.* **1987**, *109*, 3508−3513.
(13) Shin, D.-H.; Ellaboudy, A. S.; Dye, J. L.; DeBacker, M. G. *J. Phys. Chem.* **1991**, *95*, 7085−7089.
(14) Shin, D. H.; Dye, J. L.; Budil, D. E.; Earle, K. A.; Freed, J. H. *J. Phys. Chem.* **1993**, *97*, 1213−1219.

The electride K^+(cryptand[2.2.2])e^- has a similar cavity structure and a diamagnetic ground state, indicating strong coupling as in an e_2^{2-} dimer.

6. The electrides Cs^+(15-crown-5)$_2e^-$ and Cs^+(18-crown-6)$_2e^-$ are insulators or wide-gap semiconductors,[16] indicating localization of the electrons.

The experimental evidence cited above strongly favors the "stoichiometric F-center" model of electrides, with electrons trapped at all anionic sites. Of course, the electron density extends beyond the cavity boundaries. The hydrogens that line the cavities carry a partial positive charge because of the polar nature of the complexant. We anticipate overlap of the excess electron density with the hydrogens, the other complexant atoms, the cation, and neighboring electrons. Overlap of the wave functions of adjacent trapped electrons yields antiferromagnetic coupling that may be studied by magnetic susceptibility measurements. Of particular interest here is the relationship between channel geometries and electron−electron coupling.

Theoretical Considerations. Theoretical calculations support the picture of electrides given above. Exclusion of excess electron density from regions occupied by the complexed cations is of primary importance. Rencsok, Kaplan, and Harrison[17,18] carried out extensive Hartree−Fock calculations for the hypothetical molecule Li(9-crown-3)$_2$. They found that Li is converted to complexed Li^+ with the unpaired electron "squeezed out" into a Rydberg-state orbital with most of the unpaired electron density outside of the complexed lithium cation. Starting from this "expanded atom" view, one can visualize localization of the excess electron density in cavities when such molecules are brought together to form a solid. An alternative model, in which the center of "excess" electron density in Cs^+-(18-crown-6)$_2e^-$ is near the cesium,[19,20] has recently been challenged on theoretical grounds.[21]

A tight-binding (Hückel-type) calculation of the energy levels in Cs^+(18-crown-6)$_2e^-$ by Allan et al.[22] indicated that the energy of the 6s orbital of cesium lies above the bottom of the conduction band. They considered a cavity wave function for the unpaired electron to be better than occupancy of the cesium orbital.

Singh et al.[23] made extensive local density approximation calculations on Cs^+(15-crown-5)$_2e^-$. They concluded that most of the electron density is in the cavity, and that it extends into the major channel that connects adjacent cavities, providing a mechanism for electron−electron interactions. This theoretical confirmation of the importance of cavities and channels, proposed initially on the basis of the structure and properties of the first electride,[1] prompted this detailed investigation of the cavity−channel structure of electrides.

Visualization Methodology. Many computer programs are available for visualizing crystal structures. Some permit construction of "solvent accessible surfaces", regions of a crystal that allow penetration of a sphere of specified size. Von Schnering and Nesper[24] describe computer methods for displaying periodic equipotential surfaces (PEPS) that are very similar to those used here. We explored ways to easily visualize the void spaces in complex crystal structures and to determine the diameters, lengths, and geometries of channels in electrides. A brief description of the FORTRAN programs used to provide a link between structure modeling software and 3D isosurface software and their application to the cavity−channel structure of an electride has been published.[11,25] It should be noted that this procedure also provides a convenient way to visualize the shapes and dimensions of cavities and channels in complex nanoporous crystalline materials such as zeolites.[26]

Visualization of unfilled regions within a crystal was accomplished by constructing a cubic 3D grid of equally spaced points (typically 40 × 40 × 40) each carrying a number from 0 to 255 that is proportional to the distance to the nearest van der Waals atomic or molecular surface. This grid is imbedded within a collection of atomic coordinates, obtained from the crystal structure by using a commercial program such as BIOGRAF[27] or BIOSYM.[28] The rectangular coordinates in the Brookhaven Data Base format are generated from the space group, the cell dimensions, and the relative coordinates of the atoms in the asymmetric unit. Typically, 8 to 27 unit cells are included. With BIOSYM, a cubic collection of coordinates of any desired size can be directly generated. In addition to the atomic coordinates, the van der Waals radii of the atoms are included. A value of zero is assigned to any grid point that falls within the radius of an atom. When all grid points fall within the boundaries of the collection of atoms, the largest number, 255, corresponds to those grid points at which the largest possible sphere could be placed; that is, to the radius of the largest cavity. An isosurface of grid points (points with equal distance parameters) maps out the locations of the centers of spheres with the corresponding radius that would just touch the atomic surfaces. Linear 3D smoothing of the data is carried out to minimize discontinuities in the slopes of intersecting surfaces.

The results can be displayed with any program capable of 3D isosurface plots. We have used the *isosurface* routines of the AVS[29] and EXPLORER[30] programs on Silicon Graphics computers. By finding the distance parameter at which a feature just disappears it is possible to determine the maximum diameters of spheres that will just pass through the various channels and that will just fit into the cavities. In principle, a small distance parameter would give the true channel and cavity shapes, but this procedure tends to obscure interior channels and cavities by a display of those on the surface. Surface regions are distorted because of the arbitrary locations of the surface grid points with respect to the atom positions. Therefore, a compromise is reached by using a large enough distance parameter to reveal the essential void geometry at the cost of distorting somewhat the shapes and apparent sizes of the

(15) Huang, R. H.; Ward, D. L.; Dye, J. L. *J. Am. Chem. Soc.* **1989**, *111*, 5707−5708.
(16) Moeggenborg, K. J.; Papaioannou, J.; Dye, J. L. *Chem. Mater.* **1991**, *3*, 514−520.
(17) Rencsok, R.; Kaplan, T. A.; Harrison, J. F. *J. Chem. Phys.* **1990**, *93*, 5875−5882.
(18) Rencsok, R.; Kaplan, T. A.; Harrison, J. F. *J. Chem. Phys.* **1993**, *98*, 9758−9764.
(19) Golden, S.; Tuttle, T. R., Jr. *Phys. Rev. B* **1992**, *45*, 913−918.
(20) Golden, S.; Tuttle, T. R., Jr. *Phys. Rev. B* **1994**, *50*, 8059−8062.
(21) Kaplan, T. A.; Rencsok, R.; Harrison, J. F. *Phys. Rev. B* **1994**, *50*, 8054−8058.
(22) Allan, G.; DeBacker, M. G.; Lannoo, M.; Lefebvre, J. *Europhys. Lett.* **1990**, *11*, 49−53.
(23) Singh, D. J.; Krakauer, H.; Haas, C.; Pickett, W. E. *Nature* **1993**, *365*, 39−42.
(24) Von Schnering, H. G.; Nesper, R. *Angew. Chem., Int. Ed. Engl.* **1987**, *26*, 1059−1200.
(25) The programs and a description of their use are available by anonymous FTP to argus.cem.msu.edu with the path pub/dye/voids.
(26) Khan, M. I.; Meyer, L. M.; Haushalter, R. C.; Schweitzer, A. L.; Zubieta, J.; Dye, J. L. *Chem. Mater.* **1996**, *8*, 43−53.
(27) BIOGRAF, Molecular Simulations Inc., 16 New England Executive Park, Burlington, MA 01803-5297.
(28) BIOSYM, Biosym Technologies, 9685 Scranton Road, San Diego, CA 92121−2777.
(29) AVS, Advanced Visual Systems Inc., 300 Fifth Ave., Waltham, MA 02154.
(30) EXPLORER, Iris Explorer Center, 1400 Opus Place, Suite 200, Downers Grove, IL 60515-5702.

channels and cavities. A display routine, such as CorelDRAW,[31] can then be used to provide a printout of the surface picture. Either color or black and white representations may be produced. It is also possible to display the (low resolution) 3D shapes of the molecular surfaces and to combine these with cavity−channel views to form a composite image. Although the use of hard-sphere radii and the choice of van der Waals radii for the atoms are somewhat arbitrary, and smoothing may give some loss of detail, we have found these representations to be extremely useful in gaining an understanding of the void topologies in electrides. As is evident from the following discussion, a detailed knowledge of the void geometries in electrides has led to correlations between structures and properties that were not evident from the usual representations of the crystal structures.

Application to Electrides

Cs^+(15 crown-5)$_2e^-$. This is perhaps the simplest electride, with one molecule per unit cell in the $P\bar{1}$ space group,[2,32] one cavity large enough to hold a sphere of diameter 4.0 Å, and a single major channel of minimum diameter 1.5 Å and length about 4 Å. The detailed structure of the cavities and channels (Figure 1) is complex, however. Since these isosurfaces are only 0.30 Å from the atomic surfaces they show nearly the true shapes of the void spaces; the cavity−channel structure is clearly one-dimensional and the opening is continuous down the *c* axis.

The calculations of Singh et al.[23] show that the maximum unpaired electron density occurs in the cavity, but with considerable extension into the major channel along the *c* axis. Figure 2 shows the remarkable similarity between the cavity−channel structures and the electron density contours obtained from Figure 2 of ref 23. The electron density is highest where the space available is largest, as concluded by Singh et al. An interesting difference is the "bulge" in the electron density isosurface near the hydrogens of the complexant. As calculated for $Li(NH_3)_4$,[33] the partial positive charges on hydrogens tend to attract electron density. Figure 2 suggests that this also occurs in the electride Cs^+(15 crown-5)$_2e^-$.

The relative isolation of the cavities and the long, small connecting channels shown in Figures 1 and 2 are in accord with the experimental observations that Cs^+(15 crown-5)$_2e^-$ is an insulator, and that the coupling between electrons is the smallest seen in electrides. The magnetic susceptibility, χ, has a maximum at 4.3 K and follows Curie−Weiss behavior ($1/\chi$ proportional to T) above about 30 K, with a slope that corresponds to one unpaired electron per molecule.[2] Fits of the data to 3D models [2] yielded coupling constants, $-J/k_B$ of 1.6 to 1.9 K (in which k_B is the Boltzmann constant), but the fit to the data was poor. A better fit is obtained with a quasi-1D Heisenberg antiferromagnetic model, although spin anisotropy and/or other magnetic interactions are apparently not negligible.[34]

In summary, the ability to visualize the cavity−channel structure of Cs^+(15-crown-5)$_2e^-$, together with theoretical calculations, permits an understanding of the major electronic features of this electride. In addition, the anisotropy of the wave function in the excited state may be responsible for the presence of three peaks in the optical absorption spectrum.[2] The disappearance of the peak in the susceptibility when a disordered sample is thermally quenched might result from blockage of the channels by disordered complexant molecules, thus cutting off the electron−electron coupling.[35]

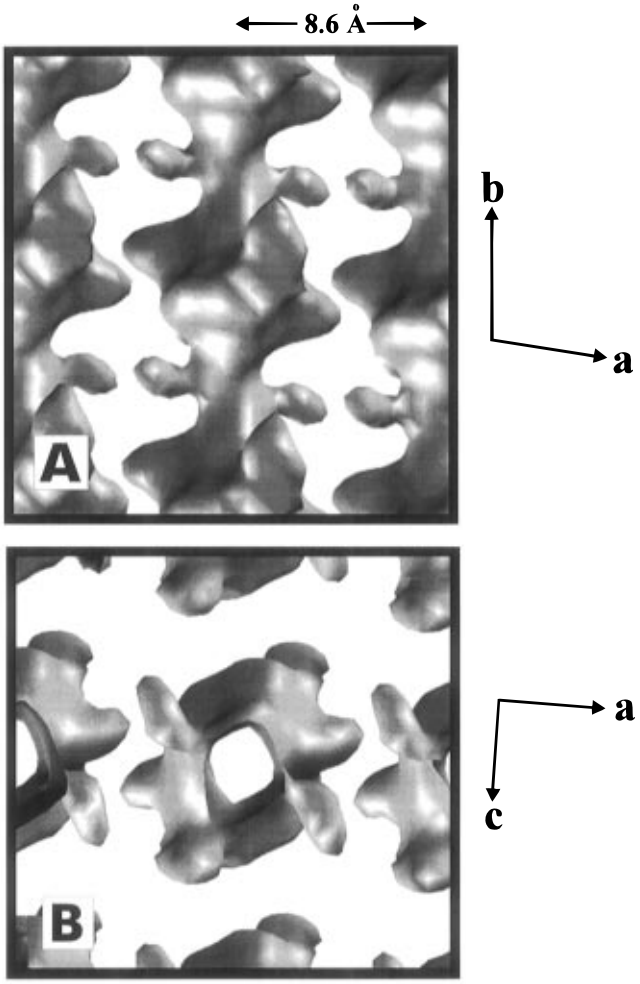

Figure 1. Two views of a cavity−channel isosurface for Cs^+(15-crown-5)$_2e^-$ at 0.30 ± 0.03 Å from the molecular van der Waals surfaces. The dark regions give the shapes of the "void" spaces in the structure; the white background represents regions occupied by molecules. In all figures, data smoothing was done, so the listed cavity−channel dimensions may have errors up to 10%, although distances indicated on the figures are accurate. Since the figures were constructed within a cubical array, the principal axis directions given may not be accurate. (A) Side view of the principal channels (diameter 1.5 Å) and the electron-trapping cavities (diameter 4.0 Å) that are 8.89 Å apart. (B) View down the *b* axis that shows the cavities, the continuous channel (white hole), and the absence of connecting channels between chains. The center-to-center distances between cavities in separate chains are 8.60 and 9.94 Å.

The views shown here should provide a starting point for theoretical calculations of the coupling between electrons and the barrier to electronic conduction along the channels. The simplest model would be a chain of spherical or ellipsoidal cavities, each containing one electron, that are connected by cylindrical tubes. It should be possible with such a collection of "particles in boxes" to calculate the expected electronic and magnetic properties.

Cs^+(18-crown-6)$_2e^-$. The seemingly simple magnetic behavior of this first crystalline electride[1] as a collection of virtually non-interacting unpaired electrons was recently shown to result from a slow, irreversible order−disorder transition at about 230 K that virtually eliminates electron−electron cou-

(31) CorelDRAW, Corel Corporation: 1600 Carling Ave., Ottawa, Ontario, Canada K1Z8R7.

(32) Ward, D. L.; Huang, R. H.; Kuchenmeister, M. E.; Dye, J. L. *Acta Crystallogr.* **1990**, *C46*, 1831−1833.

(33) Kohanoff, J.; Buda, F.; Parrinello, M.; Klein, M. L. *Phys. Rev. Lett.* **1994**, *73*, 3133−3136.

(34) Wagner, M. J.; Dye, J. L. Unpublished results.

(35) Dye, J. L. *Nature* **1993**, *365*, 10−11.

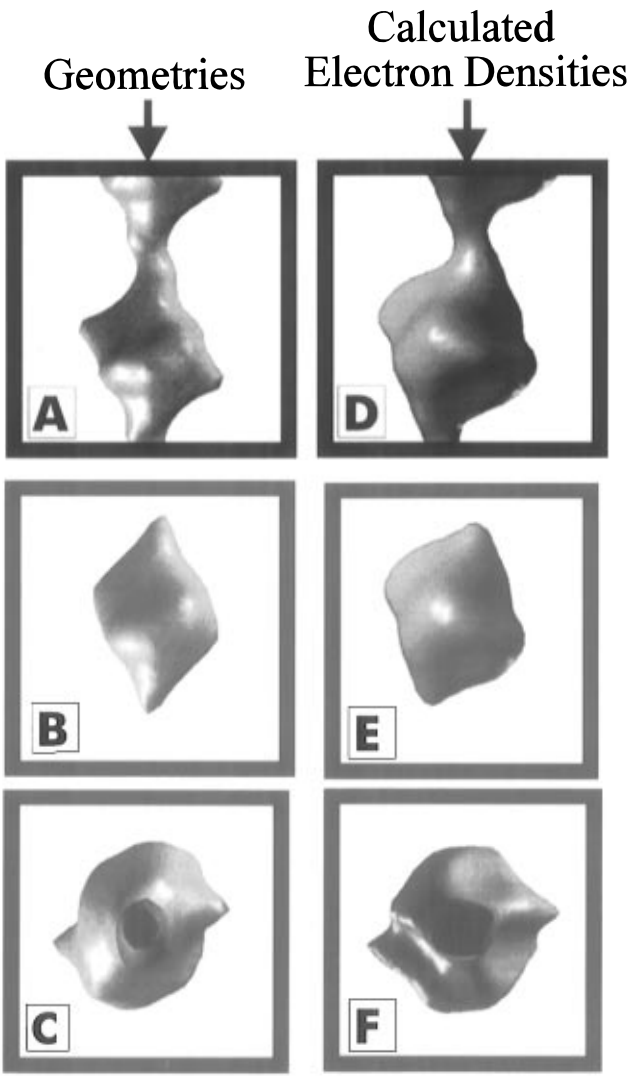

Figure 2. Geometric isosurfaces for $Cs^+(15\text{-crown-}5)_2e^-$ at 0.6 Å (A and C) and 0.85 Å (B) from the molecular surfaces. Views A and B are perpendicular to the *b* axis with the same orientation as in Figure 1, while C is down this axis. The channel down the *b* axis has a diameter at its narrowest point of 1.5 Å and is ~4 Å long. The cavities, each of which could accommodate a sphere of 4.0-Å diameter, are 8.89 Å apart along *b* and 8.60 and 9.94 Å (center-to-center) from cavities in adjacent chains. D, E, and F are corresponding views of the theoretical unpaired electron density isosurfaces of Singh *et al.* [23] Spots due to electron densities near foreground nuclei have been removed for clarity. We are grateful to D. J. Singh and W. E. Pickett for providing the data needed to generate the theoretical electron density isosurfaces.

pling.[36] Crystalline samples with the known structure have a temperature dependence of the susceptibility that can be quantitatively fit by a 1D Heisenberg antiferromagnetic chain model with the coupling constant, $-J/k_B = 38$ K.[37] The susceptibility reverts to Curie−Weiss behavior when the sample is repeatedly heated to 230−240 K. The cavity−channel structure shown here can be used to understand these effects.

Figure 3 shows two perspective views of the cavity−channel structure of $Cs^+(18\text{-crown-}6)_2e^-$. Each cavity could accommodate a hard sphere of diameter 4.8 Å. The cavities are connected along the *c* axis by short flat channels of width 1.9 Å, height ≈4 Å, and length 2−3 Å. The cavities are 8.68 Å apart (center-to-center) and each is about 6.5 Å long and 4.8 Å wide. Each cavity is connected to two cavities in adjacent chains by smaller and longer channels of minimum diameter 1.5 Å and length ≈4 Å.

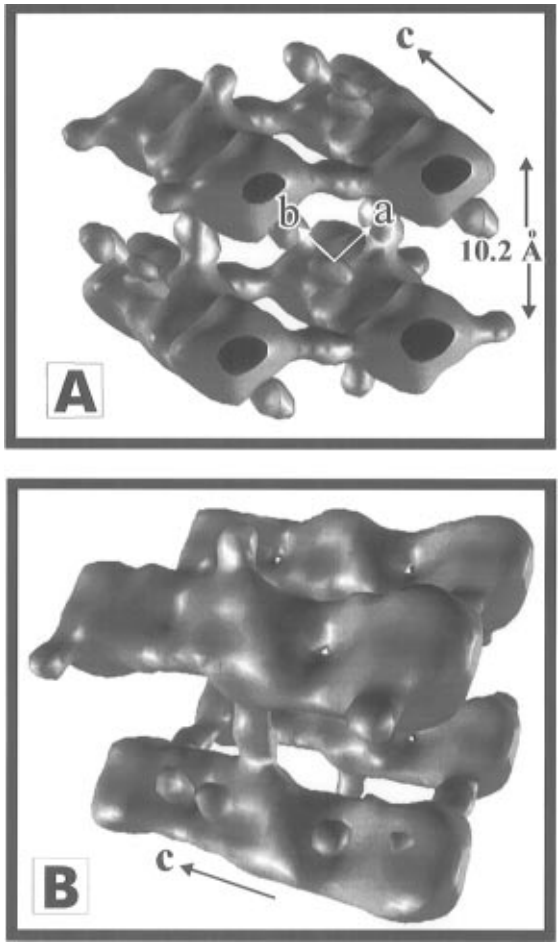

Figure 3. Two perspective views of the cavity−channel isosurfaces of $Cs^+(18\text{-crown-}6)_2e^-$ at 0.54 Å from the molecular van der Waals surfaces. Each cavity is about 6.5 Å long and 4.8 Å in diameter. Major channels are about 1.9 Å by 4 Å in cross-section and 2−3 Å long, with a pronounced "pinch" in the channel center caused by hydrogen atoms of the crown ether. Interchain channels are ≈ 1.5Å in diameter and are ≈4 Å long. Principal axis directions shown should be considered as perspective views. The cavities and channels in the center of each display are closest to the true shapes because of boundary effects, which are unavoidable in a perspective display.

The short, rather open channels explain why the electron−electron interactions in $Cs^+(18\text{-crown-}6)_2e^-$ yield a coupling constant, *J*, that is an order of magnitude larger than that of $Cs^+(15\text{-crown-}5)_2e^-$. The short channels along the *c* axis and the long, smaller interchain channels also explain the 1D Heisenberg behavior of this electride.[37] The dramatic reduction in the interelectron coupling that accompanies the order−disorder transition[36] might be caused by the "pinching-off" of the large channels in the disordered phase as the crown ether molecules reorient, with consequent reduction in overlap of the wave functions of electrons in adjacent cavities.

K^+(cryptand[2.2.2])e^-. This compound was viewed as a "dielectride" with spin-paired electrons in dumbbell-shaped cavities.[3] It was noted also that the channels between the electron-pair trapping sites are very open, so that a zigzag chain of electron-pair trapping sites is present along with smaller interchain channels to form a 2D collection of cavities and channels. After subtracting a low-temperature Curie-law "tail" (presumably from single electron defects) the susceptibility showed a slow increase with temperature that was assigned to

(36) Wagner, M. J.; Huang, R. H.; Dye, J. L. *J. Phys. Chem.* **1993**, *97*, 3982−3984.

(37) Wagner, M. J. Ph.D. Dissertation, Michigan State University, East Lansing, MI, 1994.

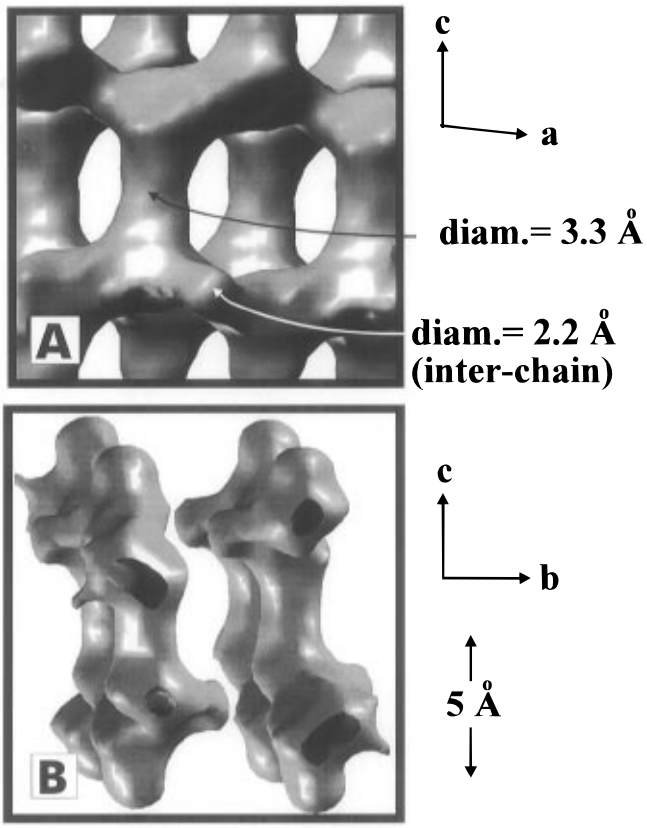

Figure 4. Electron-pair trapping centers and channels in K^+-(cryptand[2.2.2])e^-. These isosurfaces are 0.53 Å from the molecular surfaces. The complete set of cavity and channel sizes and separations are given in the text. (A) View of the major zigzag channels and U-shaped interchain connections in two adjacent planes of cavities and channels. (B) Perpendicular view showing that there are no significant channels between planes.

the population of an excited triplet state with $-J/k_B \approx 300-400$ K. Subsequent quantitative fitting by this simple model was found to be poor, however.[37] Additional higher temperature susceptibility measurements,[37] to be described in a separate publication, indicate compatibility with the alternating linear chain Heisenberg antiferromagnetic model, with coupling to the nearest electron, $-J/k_B \approx 410$ K, but also with coupling to the next-nearest electron that is 85% as large.[37]

The electrical conductivity of K^+(cryptand[2.2.2])e^- is *10 orders of magnitude larger* than those of either Cs^+(15-crown-5)$_2e^-$ or Cs^+(18-crown-6)$_2e^-$. Thin film absorption spectra[3,38] show a broad plasma-type edge, characteristic of metallic conductivity, albeit with a short mean-free path (10−20 Å).[37,39] Recent studies indicate that the observed conductivity may be due to hole defects rather than being intrinsic in nature.[39] Over the temperature range 85−230 K the ac conductivity[16] is well-described by variable-range 2D or 3D hopping.[37]

While the general features of the cavities and channels were determined from the crystal structure,[3] the present method provides a full understanding of the sizes, shapes, and connectivities of the cavities and channels. The open zigzag channels, running from top to bottom at an angle of 30° to the *c* axis, are clearly apparent in Figure 4A, as are their smaller U-shaped interconnecting channels. The offset of successive planes of channels by one-half unit is also apparent. Figure 4B shows that these planes are not connected by channels of appreciable size.

The maximum diameter of a sphere that could move through the large channels between electron pairs is 3.3 Å, while for the interchain channels it is 2.2 Å. Each cavity of a pair is 4.6 Å in diameter with centers that are only ≈5 Å apart. The minimum diameter of the "neck" between the pair is 4.0 Å. The distance between adjacent cavities in *separate* pairs along the chain is ≈7.5 Å.

The cavity−channel structure of K^+(cryptand[2.2.2])e^- provides an understanding of the strong pairwise electron coupling and the applicability of a 1D alternating Heisenberg antiferromagnetic chain model. If the electrical conductivity is due to defects such as missing electrons, one might anticipate a low barrier to motion along the chains and a higher interchain barrier. Random defect blockage along the major chains would then be compatible with a variable-range 2D hopping mechanism, while other lattice defects could lead to 3D conductivity.

Li^+(cryptand[2.1.1])e^-. This electride was prepared as a powder in 1981 and a maximum in its magnetic susceptibility was demonstrated.[40] The crystal structure and a few properties of this electride were determined some years ago, but its extreme sensitivity to thermal decomposition delayed completion of the studies, which will be described in detail in a separate publication.[41]

The major structural feature is a zigzag chain of cavities of diameter 4.4 Å connected by large open channels of minimum diameter 2.4 Å as shown in Figure 5A. Chains above and below the central chain are displaced by 1/2 unit both along and perpendicular to the chain direction. A closer isosurface (Figure 5B) shows additional channels of minimum diameter 1.5 Å that connect cavity *n* with cavities $n-2$ and $n+2$ along the chain. The intercavity distance along the most open channel between cavity *n* and cavity $n \pm 1$, 7.91 Å, is nearly the same as that between *n* and $n \pm 2$, 8.38 Å. The distance to four cavities in adjacent chains is similar, 8.15 Å. Based purely on distances then, we would expect a 3D spin system. If, however, the channels are important, we expect a "ladderlike" chain with much stronger interaction between electrons in *n* and $n \pm 1$ than those in *n* and $n \pm 2$. These interactions will "compete", since an electron in cavity *n* cannot simultaneously be opposite in magnetic orientation to those in both $n \pm 1$ and $n \pm 2$. Interactions between electrons in different chains are expected to be even weaker, since the interchain channels (not shown) have diameters below 0.95 Å.

Analytical solutions for "ladderlike" chains have not been found and extrapolations to infinite length from exact numerical calculations on finite chains fail to converge.[42] Experimentally, the magnetic behavior of this electride is complex and the studies are not yet complete. The magnetic susceptibility of one sample of quickly precipitated Li^+(cryptand[2.1.1])e^- resembles that expected for an $S = {}^1/_2$ linear chain Heisenberg antiferromagnet with a maximum at 20 K and a spin-pairing (Peierls) transition at ≈12 K.[37] More recent EPR and susceptibility data on polycrystalline samples suggest that the magnetic behavior depends on the degree of crystallinity. The origin of this effect is being investigated.

[Cs^+(15-crown-5)(18-crown-6)e^-]$_6$·(18-crown-6). This mixed sandwich electride has a very complex structure.[4] Since its cavity−channel geometry and the relation to properties are described in detail elsewhere,[11] we merely include here a picture of the complex pattern of cavities and channels that are present.

(38) DaGue, M. G.; Landers, J. S.; Lewis, H. L.; Dye, J. L. *Chem. Phys. Lett.* **1979**, *66*, 169−172.
(39) Hendrickson, J. E. Ph.D. Dissertation, Michigan State University, East Lansing, MI, 1994.
(40) Landers, J. S.; Dye, J. L.; Stacy, A.; Sienko, M. J. *J. Phys. Chem.* **1981**, *85*, 1096−1099.
(41) Huang, R. H.; Wagner, M. J.; Faber, M. K.; Ward, D. L.; Dye, J. L. Manuscript in preparation.
(42) Ananthakrishna, G.; Weiss, L. F.; Foyt, D. C.; Klein, D. J. *Physica B* **1976**, *81*, 275.

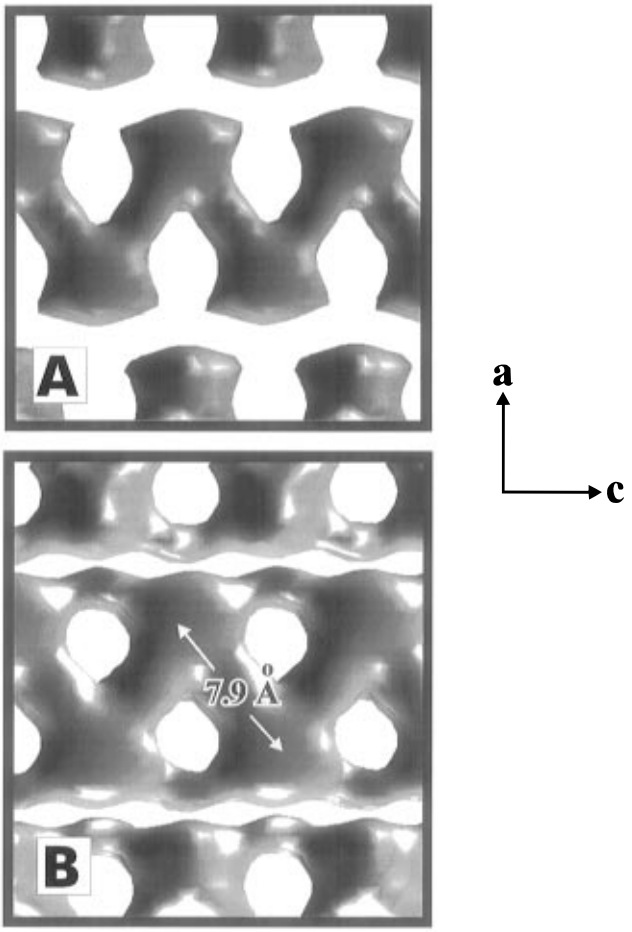

Figure 5. Cavity-channel isosurfaces of Li^+(cryptand[2.1.1])e^- at (A) 0.79 Å and (B) 0.60 Å from the atomic surfaces. The major feature shown in (A) is a zigzag chain of cavities along *c* (4.4 Å diameter) spaced 7.91 Å apart and connected by channels of diameter 2.4 Å. As shown in (B), additional channels (1.5-Å diameter) connect second-neighbor cavities. Channels (not shown) to neighboring chains have various minimum diameters, the largest of which is 0.95 Å.

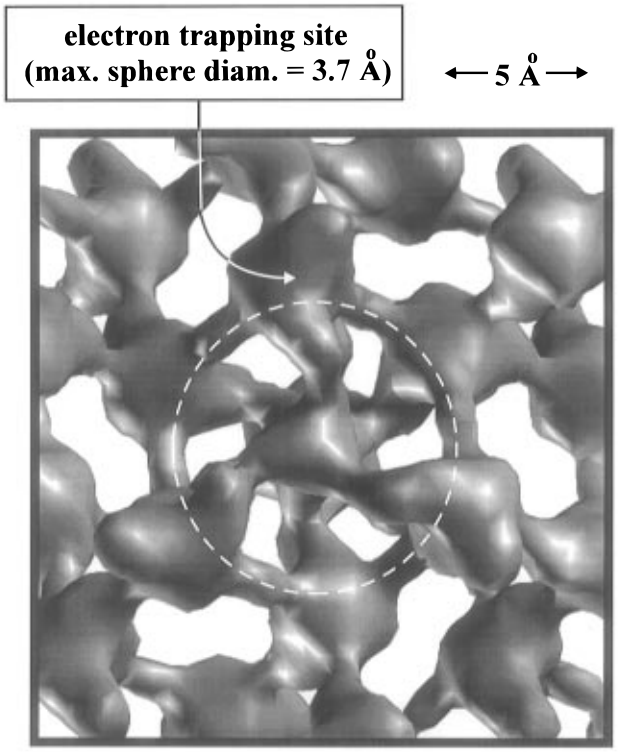

Figure 6. A view down the 3-fold symmetry axis of the complex cavities and channels in the mixed crown ether electride, $[Cs^+(15\text{-crown-5})(18\text{-crown-6})e^-]_6\cdot(18\text{-crown-6})$ at a distance of 0.55 Å from the molecular surfaces. The six cavities in the ring (dashed circle) each could contain a hard sphere of diameter 3.7 Å but obviously they are far from spherical. The central cavity (2.9-Å diamter) is empty except for the presence of some defect Cs^+ ions[4,11] and is duplicated below the central "free" crown ether. In addition, there is an empty cavity of diameter 2.9 Å situated midway between the central "free" 18-crown-6 molecules.[11] The sizes of channels between cavities are given in the text.

Figure 6 shows the ring of six large cavities, each of which could contain a hard sphere of diameter 3.7 Å connected by channels of minimum diameter 1.2 Å. The trapped electrons presumably occupy these cavities and form a six-member ring that is diamagnetic in its ground state with $-J/k_B \approx 400$ K. Each of these cavities is connected to cavities of diameter 2.9 Å above and below the central 18-crown-6 molecule by U-shaped channels of minimum diameter 1.2 Å and also with an "empty" cavity of diameter 2.9 Å situated on the 3-fold axis midway between the central 18-crown-6 molecules. In addition, each electron-trapping cavity in a ring is connected to two cavities in other rings by channels of minimum diameter 1.0 Å. An understanding of the nature of these complex electron-trapping sites, empty cavities, and connecting channels would be virtually impossible without the techniques described in this paper. The original schematic diagram of the electron-trapping cavities[4] was correct in its gross features, but lacked the detail presented here.

$Li(NH_3)_4$: Is This Compound an Electride? The crystalline metallic compound $Li(NH_3)_4$ has been known since 1968.[43] It is the lowest melting known metal (89 K) and lies just on the metallic side of the insulator−metal transition.[44] The structure of $Li(ND_3)_4$, including the positions of the D atoms, was determined in 1989 by powder neutron diffraction methods.[45] Recently, the nature of the conduction states was calculated[33] by *ab initio* density functional methods. The spatial distribution of the electron density bears a striking similarity to that of electrides, which prompted us[46] to suggest that $Li(NH_3)_4$ may be an example of a 3D metallic electride.

Figure 7A shows a perspective view of the cavities and channels in $Li(ND_3)_4$ while Figure 7B shows a closeup view. The cavities could each accommodate a hard sphere of diameter 2.6 Å and the channels have minimum diameters of 1.4 Å. The resemblance to cavity−channel views of electrides is remarkable. What makes $Li(NH_3)_4$ metallic rather than a Mott insulator? These representations suggest that it may be due to the small size of the cavities, the 3D nature of the connections, and the strong overlap of the valence electron wave functions through the short open channels.

Cesium Metal under Pressure—The Simplest Electride? Cesium metal under pressure undergoes a number of phase transitions as it gradually changes from an s-band metal to a d-band form.[47−51] At 4.3 GPa it forms the tetragonal phase Cs(IV).[48] Von Schnering and Nesper[24] conclude that partial

(43) Mammano, N.; Sienko, M. J. *J. Am. Chem. Soc.* **1968**, *90*, 6322.
(44) Stacy, A. M.; Johnson, D. C.; Sienko, M. J. *J. Chem. Phys.* **1982**, *76*, 4248−4254.
(45) Young, V. G., Jr.; Glaunsinger, W. S.; VonDreel, R. B. *J. Am. Chem. Soc.* **1989**, *111*, 9260−9261.
(46) Kaplan, T. A.; Harrison, J. F.; Dye, J. L.; Rencsok, R. *Phys. Rev. Lett.* **1995**, *75*, 978.
(47) McMahan, A. K. *Phys. Rev. B* **1978**, *17*, 1521−1527.
(48) Takemura, K.; Shimomura, O. *Phys. Rev. Lett.* **1982**, *49*, 1772−1775.
(49) Tups, H.; Takemura, K.; Syassen, K. *Phys. Rev. Lett.* **1982**, *49*, 1776−1779.

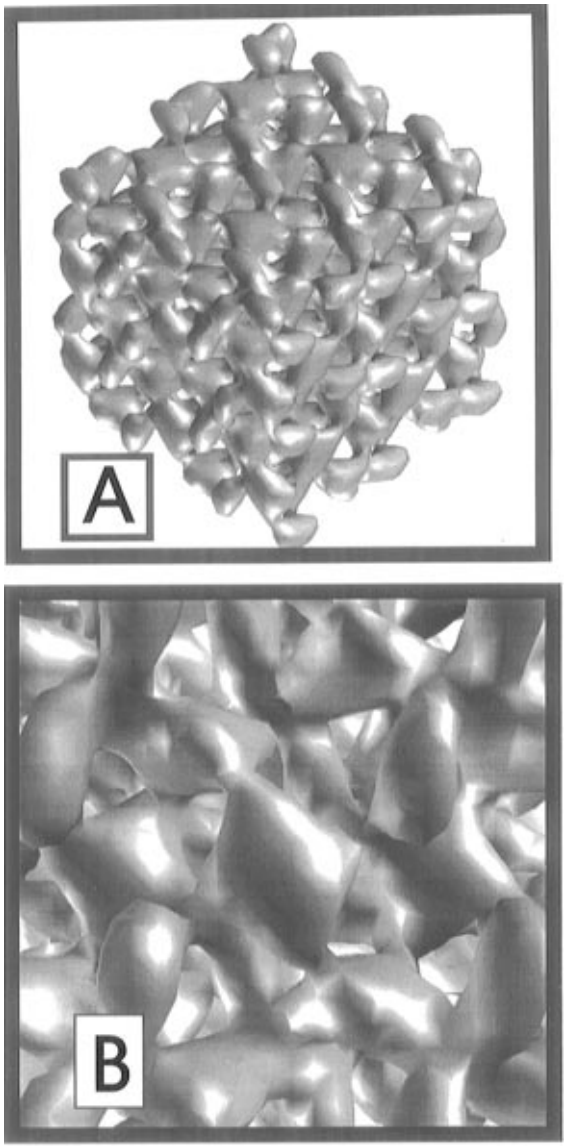

Figure 7. Two views of the cavity−channel isosurfaces at 0.6 Å from the atomic surfaces in the cubic metallic compound $Li(ND_3)_4$. View A gives an overall perspective of the 3D connectivities. View B is a closeup that displays the cavities, each of which could accommodate a sphere of diameter 2.6 Å. Each cavity is connected to four others by short (∼1 Å) channels of minimum diameter 1.4 Å.

localization of the valence electron density occurs, not in proximity to the Cs core, but rather in bent tubes at the square faces and centers of the trigonal prisms formed by the packing of the cesiums. Indeed, they view "this Cs modification as cesium electride, Cs^+e^-"! These authors[24] present a graphical representation of the 3D distribution of Cs^+ ions and the periodic zero potential surface (POPS) that is of essentially the same geometry as we obtain from the void volume outside of the van der Waals Cs^+ spheres in this structure. Figure 8 shows two views of the spatial distribution of cavities and channels in Cs(IV). As one would expect from the similarity of the methods used, the 2.3-Å-diameter cavities at the centers of the square faces within the trigonal prisms and the large (1.7- and 1.9-Å diameter) channels that connect the cavities to form a 3D array bear a strong resemblance to the POPS display of Von Schnering and Nesper.[24]

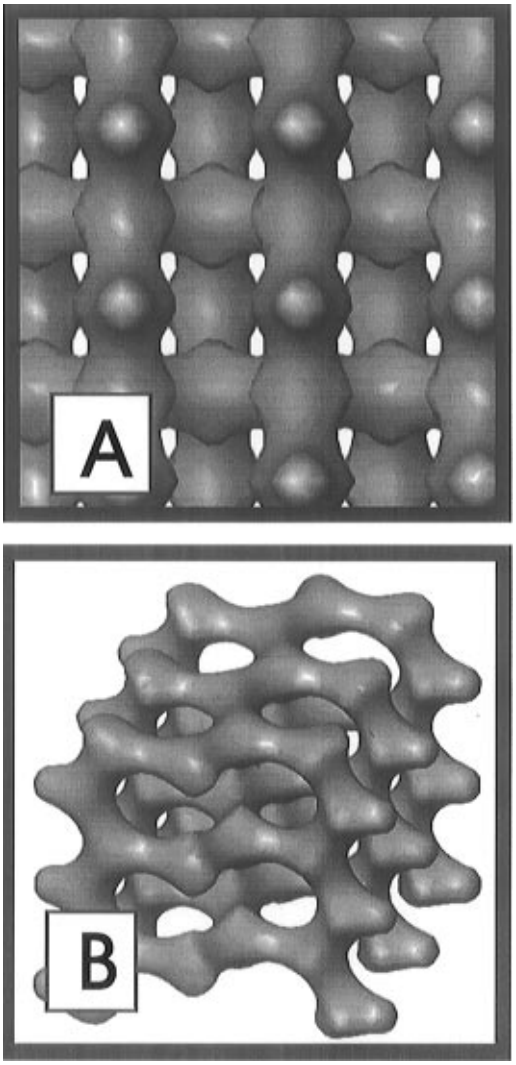

Figure 8. Views of the void spaces in the high pressure phase, Cs-(IV), of cesium metal[48] that has been referred to as an electride.[24] View A is down the *c* axis at 0.6 Å from the van der Waals surfaces of the Cs^+ ions. Each cavity has a diameter of 2.3 Å and the connecting channels shown have minimum diameters of 1.9 Å. Channels perpendicular to this view have minimum diameters of 1.7 Å. View B is a perspective view of the cavities and channels that demonstrates the 3D connectivity of the void spaces.

Conclusions

The electron distribution in electrides is topologically complex so that high-quality theoretical treatments are very difficult. We present here a simplified view of electrides that emphasizes their cavity−channel structure. We propose that, to first order, electron density distributions in electrides resemble the available void space to provide "electron lattice gases" with known geometries. The differences in magnetic and electronic behavior from one electride to another can be rationalized in terms of the sizes and distributions of cavities and the diameters and lengths of the connecting channels. These views may also be used as the starting point for approximate theoretical treatments of electronic coupling, spectra, and barriers to conduction in electrides. They may also prove useful in synthesis. It is easier to synthesize alkalides than electrides and to determine their crystal structures. By deleting the alkali metal anion from a representation of the structure, we can approximate the expected cavity−channel structure of the corresponding electride and thus decide on which electride targets to focus our efforts. If the correlations presented here have general validity, we should also

(50) Takemura, K.; Shimomura, O.; Fujihisa, H. *Phys. Rev. Lett.* **1991**, *66*, 2014−2017.
(51) Abd-Elmeguid, M. M.; Pattyn, H.; Bukshpan, S. *Phys. Rev. Lett.* **1994**, *72*, 502−505.

be able to predict the magnetic coupling and dimensionality of the target electrides.

The representations of both $Li(ND_3)_4$ and Cs(IV) raise the question, "What is an electride?" Both are metallic and the electronic properties can be well-described by band structure calculations in which there is no gap at the Fermi surface. All five of the electrides that have complexed cations are essentially ionic compounds in which localized electrons serve as the anions. They, therefore, can logically be called electrides. But there is evidence that hole-doping of K^+(cryptand [2.2.2])e^- converts it to a 1D metal with activated hopping to form a 2D conductor. Thus, the terms "electride" and "metal" need not be mutually exclusive. The representations displayed in this paper make it clear that the topology of the void spaces cannot be *directly* used to separate electrides from ordinary metals. Theoretical treatments of the interactions among electrons in distinct cavities are needed to distinguish among insulating electrides, metallic electrides and normal metals.

Acknowledgment. This research was supported in part by NSF Solid State Chemistry Grant No. DMR 94-02016 and by the Michigan State University Center for Fundamental Materials Research. The development of the display methodology was supported in part by AFOSR Grant No. F49620-92-J-0523. We thank Thomas Atkinson, Paul Reed, and David Young for assistance with computer program development and use.

JA960548Z